Distant origins of Arctic black carbon: A Goddard Institute for Space Studies ModelE experiment

Dorothy Koch and James Hansen

NASA Goddard Institute for Space Studies, Columbia University, New York, New York, USA

Received 29 July 2004; revised 22 November 2004; accepted 17 December 2004; published 25 February 2005.

[1] Black carbon (BC) particles, derived from incomplete combustion of fossil fuels and biomass, may have a severe impact on the sensitive Arctic climate, possibly altering the temperature profile, cloud temperature and amount, the seasonal cycle, and the tropopause level and accelerating polar ice melting. We use the Goddard Institute for Space Studies general circulation model to investigate the origins of Arctic BC by isolating various source regions and types. The model suggests that the predominant sources of Arctic soot today are from south Asia (industrial and biofuel emissions) and from biomass burning. These are the primary global sources of BC (approximately 20% and 55%, respectively, of the global emissions), and BC aerosols in these regions are readily lofted to high altitudes where they may be transported poleward. According to the model the Arctic BC optical thickness is mostly from south Asia (30%) and from biomass (28%) (with slightly more than half of biomass coming from north of 40°N); North America, Russia, and Europe each contribute 10–15%. Russia, Europe, and south Asia each contribute about 20–25% of BC to the low-altitude springtime "Arctic haze." In the Arctic upper troposphere/lower stratosphere during the springtime, south Asia (30–50%) and low-latitude biomass (20–30%) are dominant, with a significant aircraft contribution (10–20%). Industrial S emissions are estimated to be weighted relatively more toward Russia and less toward south Asia (compared with BC). As a result, Russia contributes the most to Arctic sulfate optical thickness (24%); however, the south Asian contribution is also substantial (17%). Uncertainties derive from source estimates, model vertical mixing, and aerosol removal processes. Nevertheless, our results suggest that distant sources contribute more to Arctic pollution than is generally assumed.

Citation: Koch, D., and J. Hansen (2005), Distant origins of Arctic black carbon: A Goddard Institute for Space Studies ModelE experiment, *J. Geophys. Res.*, *110*, D04204, doi:10.1029/2004JD005296.

1. Introduction

[2] The Arctic is a particularly sensitive region to global climate change. Observations and models indicate that as the climate warms, the Arctic warms most and fastest [e.g., *Manabe et al.*, 1992]. Sea ice and snow cover there are decreasing. Changes on Greenland can have global effects via changes in sea level. The Arctic climate has a complex meteorological system, including formation of a strong polar vortex during winter with relatively stable stratification in the troposphere. When the polar vortex weakens in springtime, the vertical stability breaks down allowing greater exchange with upper level air. Transport into the Arctic is affected by the location and strength of the polar front as indicated by the Arctic Oscillation [*Hodges*, 2000], which is correlated with the North Atlantic Oscillation [*Wallace and Thompson*, 2002]. The Arctic climate is especially sensitive to changes in the hydrological cycle, including river influx, ice, snow and permafrost amounts and cloud formation and temperature [e.g., *Vorosmarty et al.*, 2001]. Changes in Arctic chemistry and influx of pollution may disrupt this sensitive system [e.g., *Rinke et al.*, 2004]. We do not attempt to address the complex web of dynamical and radiative influences. Our focus is on black carbon aerosols in the Arctic as we attempt to discern its origins.

[3] Black carbon (BC), which is the absorbing portion of carbonaceous aerosols, commonly called "soot," is derived from the incomplete combustion of fossil fuels (primarily coal and diesel) and from the burning of biomass or biofuels. Globally it may contribute to climate warming, with recent radiative forcing estimates of +0.55 W m^2 [*Jacobson*, 2001] or higher if various indirect effects are considered [e.g., *Hansen and Sato*, 2001; *Hansen et al.*, 2002]. BC has been implicated in previous studies as potentially disrupting Arctic climate. *Clarke and Noone* [1985] found that snow albedos are reduced by 1–3% in fresh snow and by another factor of 3 as the snow ages and the BC becomes more concentrated. *Hansen and Nazarenko* [2004] modeled this decreased albedo in Arctic snow and sea ice and found this resulted in a hemispheric radiative forcing of +0.3 W m^{-2}, which may have had a substantial impact on the Northern Hemisphere climate in recent

0148-0227/05/2004JD005296$09.00

decades. In addition, soot in the air may absorb radiation, warming the air and possibly reducing cloud formation [*Ackerman et al.*, 2000; *Hansen et al.*, 1997].

[4] Most aerosols are believed to be transported to the Arctic during the winter and spring via the mostly low-altitude 'Arctic haze' transport events [*Shaw*, 1995]. Arctic haze is associated with (otherwise) clear, typically anticyclonic conditions. The haze consists primarily of particles, characterized by high sulfur concentrations and other components such as soot. At the surface, particulate concentrations are maximum during winter and springtime, due to a combination of more efficient poleward transport during these seasons and increased removal by low-level drizzling clouds in the summer [*Shaw*, 1995; *Barrie*, 1986]. Sulfate amount tends to peak slightly later in winter than black carbon, because sulfate formation depends upon photo-oxidants that become available when the polar sun rises [*Hopper et al.*, 1994]. *Rahn* [1981a, 1981b] used chemical fingerprinting of the wintertime low-altitude haze to identify likely source regions. The high observed Mn/V and elevated black carbon concentrations point to Eurasia rather than North America as the likely major source area. However the North American Arctic had Mn/V too high to be attributed to either region. *Rahn* [1981b] suggested coal burning from central USSR as a likely source of such very high Mn/V. China and south Asia were excluded from the analysis on the basis of meteorological argument. For example, air masses from the south of Barrow (the presumed pathway for south Asian airmasses) were observed to be much cleaner than those from the north. More sophisticated analyses, using more elements [*Rahn and Lowenthal*, 1984; *Lowenthal and Rahn*, 1985; *Lowenthal and Borys*, 1997] and incorporating trajectory information [*Cheng et al.*, 1993] confirmed Eurasia as the primary source of winter-spring Arctic haze. Once again China and south Asia were not included in these analyses since they were assessed to be unlikely source regions.

[5] Meteorological conditions and backtrajectory analysis have generally supported the northern Eurasian source region of Arctic haze. The midnorthern Eurasian high, aided by cyclonic systems over the Barents Sea, steers pollution from Eurasia into the Arctic. *Iversen and Joranger* [1985] argued that the formation of a large isentropic dome that extends over Eurasia during winter facilitates transport of pollution poleward. However, some recent analyses leave open the possibility of south Asian pollution sources. *Harris and Kahl* [1994] analyzed isentropic back trajectories for 7 years of data at Barrow, Alaska. They showed that during the Arctic haze season, transport from north central Russia occurs near the surface with about 20% frequency. Less frequent (10%) transport from Europe occurs at higher altitude. Interestingly, over 30% frequency of transport originates from the North Pacific, at altitudes of 1500–3000 m. *Khattatov et al.* [1997], examined lidar measurements throughout the Arctic, and suggested that 5-day back trajectories typically found air masses still within the Arctic vortex rather than near their source regions. They argued that Arctic haze appears to come from aloft rather than being transported near the surface.

[6] Chemical modeling studies [e.g., *Klonecki et al.*, 2003; *Lamarque and Hess*, 2003; *Stohl et al.*, 2002] found that although south Asia generates significant amounts pollutants such as ozone, CO and hydrocarbons, it is not an important source region to the Arctic.

[7] Thus, on the basis of analysis of trace elements, meteorology, back trajectory and chemistry models, it appears that Eurasia (western Asia and eastern Europe) is the primary source of Arctic haze, defined to be the particulate pollution near the surface of the Arctic during winter and spring. However, when considering the origin and impacts of black carbon in the Arctic, several factors not usually included in Arctic haze studies need to be considered.

[8] First are some of the distinct characteristics of black carbon. Most industrial and biofuel BC emissions are presently derived from south Asia [*Bond et al.*, 2004]. BC emissions, compared with sulfate, are more heavily weighted toward south Asia. BC also has a relatively large source from tropical biomass burning, again weighting its global emissions southward. In contrast with less soluble gaseous pollutants, particulates are more likely to be deposited (mostly rained out) when they are confined to the lower troposphere, as emissions from Europe and Russia commonly are. However particles from East Asia are more readily lofted to higher altitudes where they can travel greater distances above precipitating clouds.

[9] Thus, if these distant sources are substantial contributors to the Arctic, we would expect to find evidence in high altitude haze. Such higher altitude pollution would be less limited to the winter/spring, but would also appear later in the year. As mentioned above, *Khattatov et al.* [1997] inferred significant high altitude haze. If haze is derived from south Asia, one would expect it to appear in the North Pacific at high altitudes, a frequent transport pathway throughout the year [*Harris and Kahl*, 1994]. Several aircraft studies have reported high altitude summertime haze. For example, *Brock et al.* [1989] reported substantial summertime haze during August 1985 above 850 mbar over Greenland and the North American Arctic. The haze particles were primarily sulfate and soot was also present. The authors note that such summertime haze is often not visible from the surface because of the frequent presence of low-level clouds in summer. *Scheuer et al.* [2003] observed the progression of particulate sulfate vertical distribution from spring into summer (2000) over the North American Arctic. During early winter the haze was confined to the surface. As the season progressed surface haze diminished and high altitude haze increased. *Rosen and Hansen* [1984] report that BC in aircraft observations over Barrow increase by a factor of 3 above the boundary layer. Other areas of the Arctic also have distinct layers of high BC concentration, often with substantial levels in the free troposphere.

[10] We should also bear in mind that the relative emissions from potential source regions have shifted over the course of the past 40 years, since the early investigations of Arctic haze. *Novakov et al.* [2003] have estimated industrial changes in BC emissions for some countries, on the basis of fuel use and limited consideration of technology change. The (former) Soviet Union (FSU) was implicated as a major source of Arctic haze in many studies. *Novakov et al.* [2003] found that black carbon emissions from the FSU in the late 1990s was less than 1/4 their peak levels of 1980. European emissions are also about 1/3 their levels in the 1970s. However China and India have doubled their BC emissions

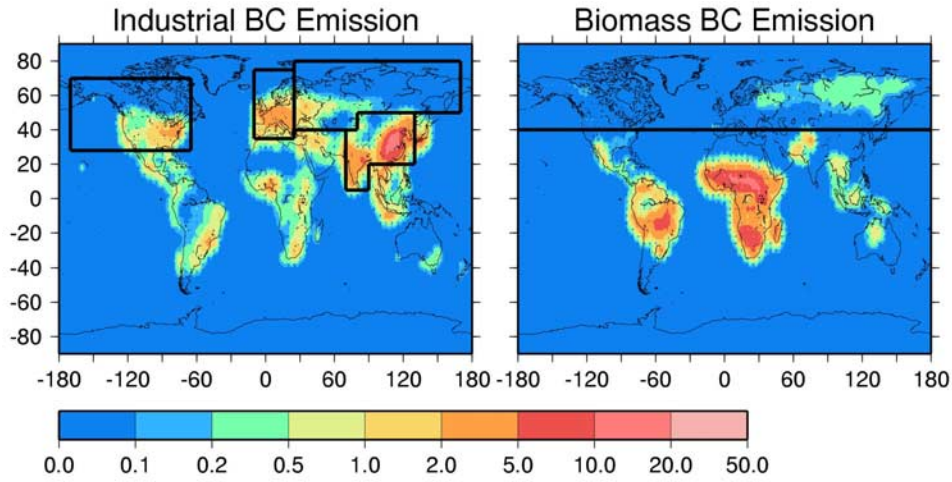

Figure 1. Industrial and biomass black carbon emissions (ng C m^{-2} s^{-1}) with boxed areas showing regions assumed in the model experiments.

since the late 1970s. Thus BC emissions are more heavily weighted toward south Asia than they were in the 1970s and 1980s, when many of the Arctic haze studies took place. A recent analysis of long-term BC concentrations at Alert show a 55% decline since the late 1980s [*Sharma et al.*, 2004]. This decline appears to be correlated with decreased emissions from the FSU.

[11] Several studies, focused more on the outflow from Asia, hint at a potentially significant role for East Asian pollution in the Arctic. *Wilkening et al.* [2000] reported a significant level of east Asian pollution transported across the Pacific to North America and suggested that this may be an important Arctic source as well. Where there is Asian dust, there is often black carbon, as reported by *Perry et al.* [1999] who frequently observed black carbon mixed with dust, and sometimes independent of dust, over Hawaii in the springtime. *Kaneyasu and Murayama* [2000] reported very high levels of BC (>150 ng m^{-3}) in the north central Pacific. The BC was associated with high levels of sulfate and not with potassium, indicative of a coal burning source rather than a biomass source. Their analysis indicated that it was derived from Asia, lofted to high altitudes, transported out over the Pacific, where it descended to the surface. A similar transport pathway was presented by *Raatz* [1985]. *VanCuren and Cahill* [2002] found substantial levels of Asian dust in decade-long records at elevated sites in North America. They argued that the dust is transported steadily, during all seasons except winter, at altitudes of 500–3000 meters. After further analysis of the data, *VanCuren* [2003] found the Asian dust is mixed with substantial amounts of combustion products, including elemental carbon. The export of pollutants from Asia has been the topic of recent campaigns, such as the spring 2001 ACE Asia (Aerosol Characterization Experiment) and the spring 2002 NOAA-ITCT 2K2 (Intercontinental Transport and Chemical Transformation 2002) project. During the NOAA-ITCT 2K2, rapid transport of high altitude (>2 km) Asian urban and biomass pollutants and particles across the Pacific was reported [*Bertschi et al.*, 2004]. *Matsuki et al.* [2003] used aircraft, lidar and trajectory analysis, and *Liang et al.* [2004] used the GEOS CHEM model, to show that during winter the transport appears to be facilitated by uplift ahead

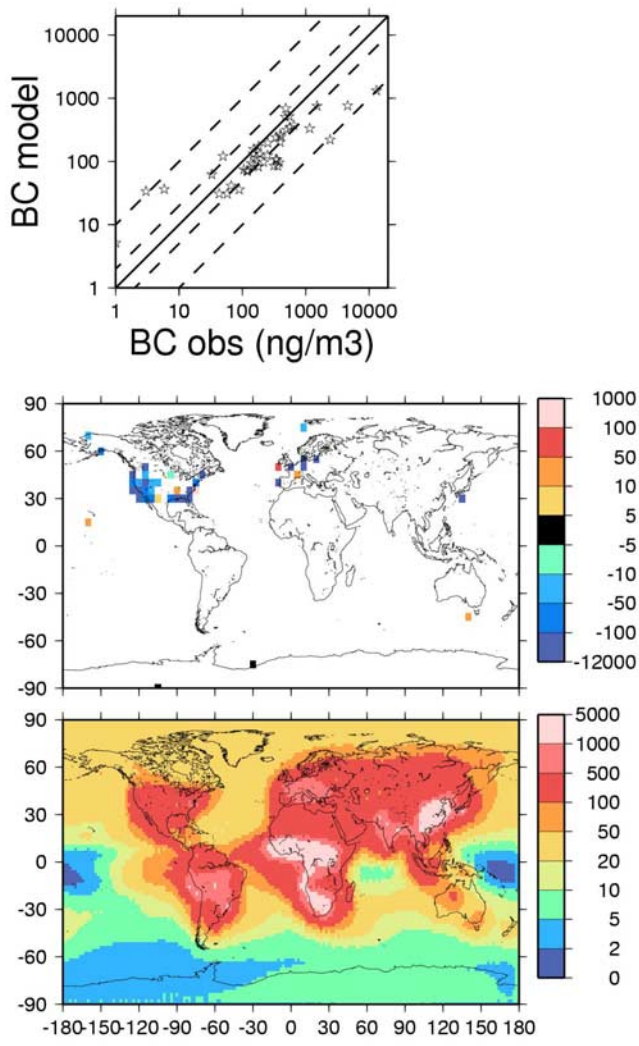

Figure 2. (top) Scatterplot of observed and modeled black carbon annual mean surface concentrations, with factors of 2 and 10 difference (dashed lines); (middle) difference between observed and modeled concentrations; and (bottom) model surface concentration. Units are ng m^{-3}.

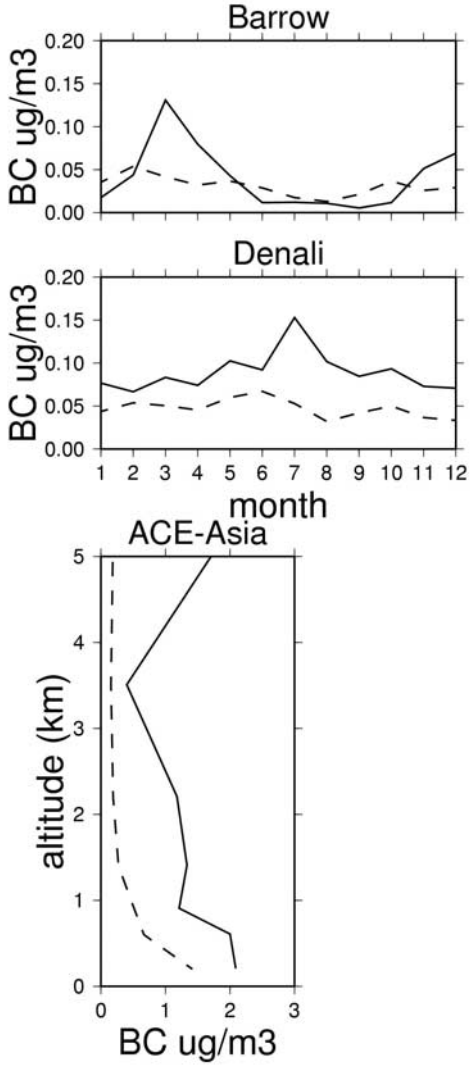

Figure 3. Seasonality of observed (solid curve) and modeled (dashed curve) BC surface concentration at (top) Barrow and (middle) Denali, Alaska. (bottom) Comparison of model with ACE-Asia aircraft measurements ($\mu g/m^3$). The model results are for April at the points corresponding to the measurement locations. The observed concentration at 5 km is based on only two measurements.

of cold fronts and rapid transport by westerlies; during summer convective uplift also lofts pollution from the boundary layer. During springtime this transport occurs throughout the column primarily between 20–50°N; during summer the transport shifts to higher levels (>2–4 km) and to higher latitudes, 30–60°N. During ACE Asia, *Cahill* [2003] used elemental analysis and back trajectory to demonstrate the transport of Asian aerosols into Alaska and the sub-Arctic. *Biscaye et al.* [2000] also reported large amounts of Asian dust transported from Asia across North America, with a reduction of less than a factor of 10 as it crosses North America en route to Greenland. They postulated that Asian aerosol pollutants should have a similar fate. Indeed, significant Asian dust, along with background pollution, was observed in the Arctic during the spring of 1976 [*Rahn et al.*, 1977].

[12] *Bowling and Shaw* [1992] used thermodynamical argument to indicate that in order for polluted air to reach the Arctic via isentropic flow, low-level haze probably needs to originate from smoke stack injections into dry air; higher-level haze (above 3 km) would need to come from an extremely dry and/or high altitude source, such as a desert. This analysis might be consistent with a mixed dust-pollution source region such as the Asian Steppes. Hot dry biomass burning conditions might also satisfy the thermodynamic requirements.

[13] We use our global model to examine the degree to which the Arctic is impacted by the more distant south Asian and low-latitude biomass regions which have the largest emissions, compared with the previously studied "Arctic haze" source regions of Europe, Russia and North America.

2. Model Description

[14] We use the new "modelE" version of the Goddard Institute for Space Studies (GISS) general circulation model (GCM). This version of the GCM is described by G. A. Schmidt et al. (Present-day atmospheric simulations using GISS ModelE: Comparison with in situ, satellite, and reanalysis data, submitted to *Journal of Geophysical Research*, 2004) and the modelE sulfate and sea salt aerosol simulations are described by D. Koch et al. (Sulfur, sea salt, and radionuclide aerosols in GISS modelE, submitted to *Journal of Geophysical Research*, 2005, hereinafter referred to as Koch et al., submitted manuscript, 2005). We use a 20 layer version with model top at 0.1 mbar and moderate boundary layer resolution (layer 3 is centered at 909 mbar). Horizontal resolution is $4° \times 5°$.

[15] As detailed by Koch et al. (submitted manuscript, 2005), the resistance-in-series dry deposition scheme is now more tightly coupled to the GCM boundary layer (compared with *Koch* [2001]). In addition the model now has a prognostic cloud-water budget for dissolved species so that the species are held along with the cloud water until evaporation or precipitation either returns them to the cloud-free portion of the grid box or rains them out.

[16] We carry 3 black carbon aerosol tracers: an insoluble industrial BC, a soluble industrial BC and a biomass BC. All industrial BC (except aircraft) is assumed to be insoluble when emitted and then is aged to become soluble, assuming an *e*-fold time of 1 day. Biomass burning BC is usually coemitted with some soluble components, so it is assumed to be partially (60%) soluble. In order to prevent excessive BC in the upper troposphere, we enhance the convective scavenging for partially soluble or insoluble particles and assume that a particle's convective solubility

Table 1. BC Emission Regions

Region	Tg yr^{-1}	Percent	Burden, Tg	Percent
Globe	10.68	100	0.222	100.0
Biomass south of 40°N	5.68	53	0.128	57.7
Biomass north of 40°N	0.32	3	0.007	3.2
South Asia	2.08	19	0.046	20.7
Europe	0.47	4	0.008	3.6
North America	0.39	4	0.007	3.2
Russia	0.21	2	0.005	2.2
Aircraft	0.01	0	0.003	1.3
Rest of world	1.53	15	0.017	7.7

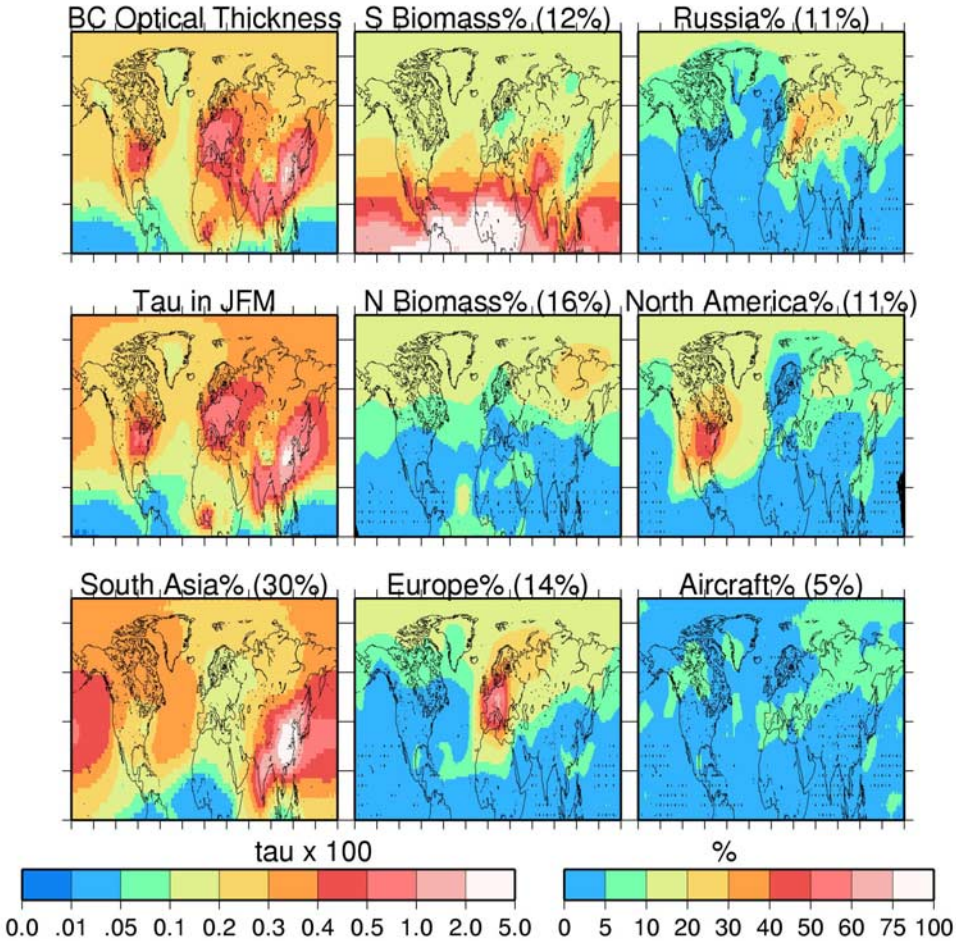

Figure 4. Northern Hemisphere (top left) black carbon optical thickness annual average, (middle left) τ during January–March ($\times 100$), and the percent contributions to BC τ based on regional source experiments. S and N biomass are for biomass emissions south and north, respectively, of 40°. Numbers in parentheses are average percent contribution to BC τ in the Arctic.

is the average between the assumed (stratiform cloud) solubility fraction and 1. In a previous model version [*Koch*, 2001] 100% aerosol solubility during convection was assumed since aircraft measurements indicated that BC concentrations in the upper troposphere should be very low. However these measurements may have been unrealistically low [*Baumgardner et al.*, 2004] so we decrease convective scavenging here. For ice clouds we permit 5% of the solubility assumed for liquid clouds.

[17] Industrial black carbon emissions are from *Bond et al.* [2004] and include both fossil fuel and biofuel. Biomass burning emissions are from *Cooke and Wilson* [1996] and these emissions are distributed throughout the boundary layer. Aircraft emissions are based on the fuel emissions of *Baughcum et al.* [1993] with an assumed BC emission rate of 0.04 g/kg fuel [e.g., *Intergovernmental Panel on Climate Change*, 1999]. The global distribution of emissions is shown in Figure 1.

3. Model Results

[18] The model's global BC burden is 0.22 Tg C with an average lifetime of 7.3d. Black carbon removal is about 70% by wet deposition and 30% by dry deposition.

[19] In order to assess the model's ability to simulate BC we compare it with annual average surface concentration observations in Figure 2. The observations include data collected after the late 1980s, with duration of at least 1 year. We make use of data referenced by *Liousse et al.* [1996], *Cooke et al.* [2000], *Koch* [2001], and the United States 1995–2002 data from the Interagency Monitoring of Protected Visual Environments (IMPROVE, http://vista.cira.colostate.edu/improve). This model simulation agrees better with observations than the model results of *Koch* [2001]. This is because we have eliminated old and short-duration data and because of the new industrial emission inventory. As in work by *Koch* [2001] and typical of other global models, the model generally has less BC than is observed; however most points lie within a factor of 2 of the observed values. Note that both of the annual mean points in the Arctic are less than the observations.

[20] Since we are focusing on transport to the Arctic, we show in Figure 3 a comparison of model with seasonal BC surface concentration data from Barrow, Alaska (71.2°N 156.3°W), for the year 1989 [*Bodhaine*, 1995] and from Denali AK (63.7°N 149.0°W; IMPROVE network) for 1988–2002. Barrow shows the observed winter and spring peaks expected for Arctic haze. The model fails to capture

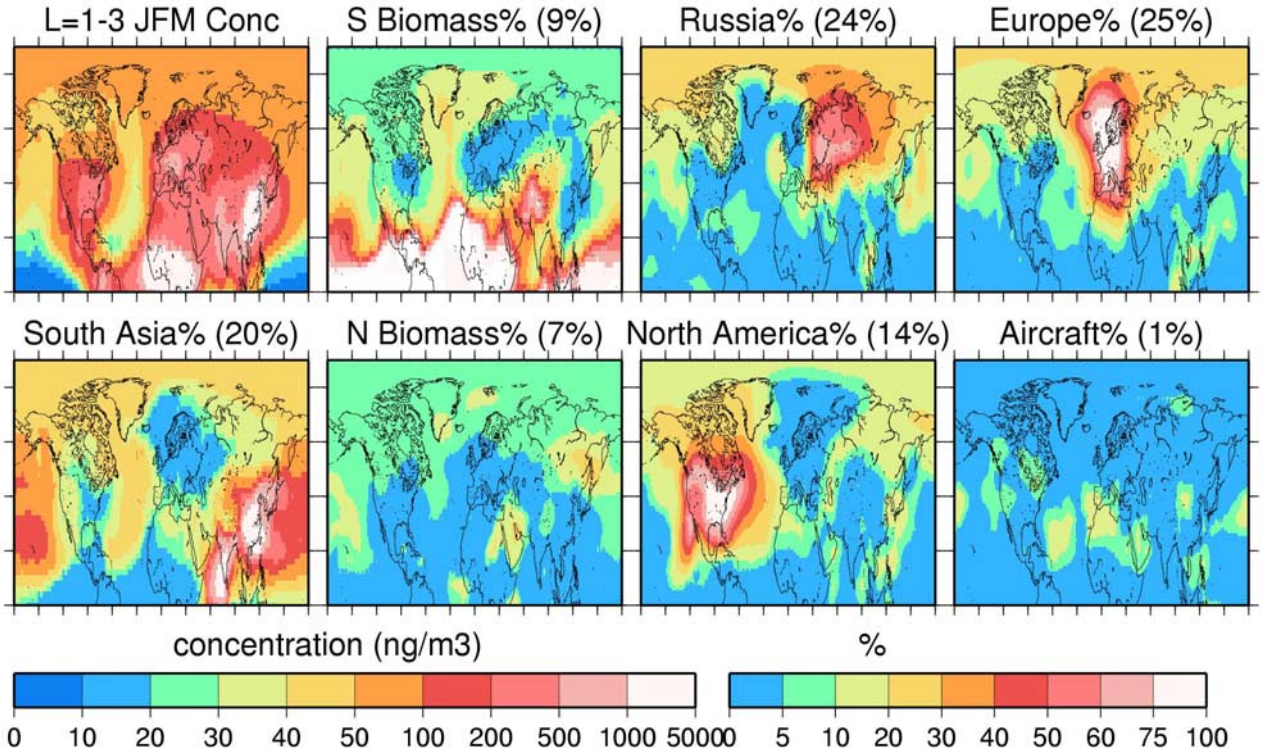

Figure 5. (top left) January–March surface (model layers 1–3) black carbon concentration (ng m^{-3}) and percent contributions from regional experiments. Numbers in parentheses are average percent contribution to BC concentration in lowest three layers in the Arctic.

this peak, however the seasonality is stronger in other parts of the Arctic, as we will see below. To some degree the model's inability to capture the peaks may be related to our lack of seasonality in emissions. *Streets et al.* [2003] showed that residential BC emissions from China have considerable seasonality, so that winter BC emissions are about double those in summer. An additional difficulty is that the model precipitation over China is excessive in winter and spring, so that the BC is deposited prior to leaving the region. Denali is in southern Alaska and its BC concentration is higher than at Barrow. BC at Denali does not peak in springtime as the typical Arctic haze does. During the 1990s there was minimal seasonality in BC at Denali. In more recent years (2000–2002) BC peaked during summertime. Sulfate at Denali usually peaked in winter-spring during the 1990s; however its peak has also shifted somewhat toward summer in recent years. The model has moderate seasonality that is highest in spring and summer and the BC is less than observed. The same aerosol model is quite successful at modeling sulfate in the Arctic (Koch et al., submitted manuscript, 2005), with peak concentrations in winter-spring as observed. In Denali Alaska the modeled sulfate peaks in late spring, in excellent agreement with the recent observations there. In Iceland the modeled sulfate is too small, however the seasonal cycle is realistic. Thus it appears that the model does generate the Arctic haze peak for other species and in other regions of the Arctic. Overall it appears that the model does not transport enough BC to the Arctic. However it is difficult to assess the model seasonality, since the seasonality at Barrow may be changed since 1989, as at Denali.

[21] Also shown is a comparison of model with ACE-Asia aircraft data [*Huebert et al.*, 2004], east of Asia in late March to early June 2001. The average over the observed points is 1.8 and the average of the corresponding model points is 0.9, suggesting that the model emissions may be too low in this region. Also, the model BC is removed by excessive springtime precipitation in the model over China.

3.1. Regional Experiments

[22] In order to investigate the impact of various emission regions and types we performed 6 experiments in which we turned off individual source regions. The first experiment includes all emissions, with industrial and biomass black carbon as distinct tracers. In experiments 2–5 we turned off industrial emissions in regions roughly corresponding to North America, Europe, Russia, and south Asia (including China and India), and in experiment 6 we turned off the aircraft emissions. In a 7th experiment we turned off biomass burning north of 40°N. This allows us to distinguish between "northern" biomass emissions (i.e., north of 40°N) and "southern" biomass (i.e., south of 40°N). We do the experiments by elimination in order to minimize the disruption to the climate, since the aerosols are permitted to impact the model's radiative balance. The regions are shown in Figure 1 and the emission amounts and percentages are listed in Table 1. We emphasize that the regions are approximate and do not exactly correspond to their geographic labels. Note that by far the largest industrial BC emissions are from south Asia.

[23] Table 1 also shows the various regional contributions to the total BC burden. We see that for some regions (e.g.,

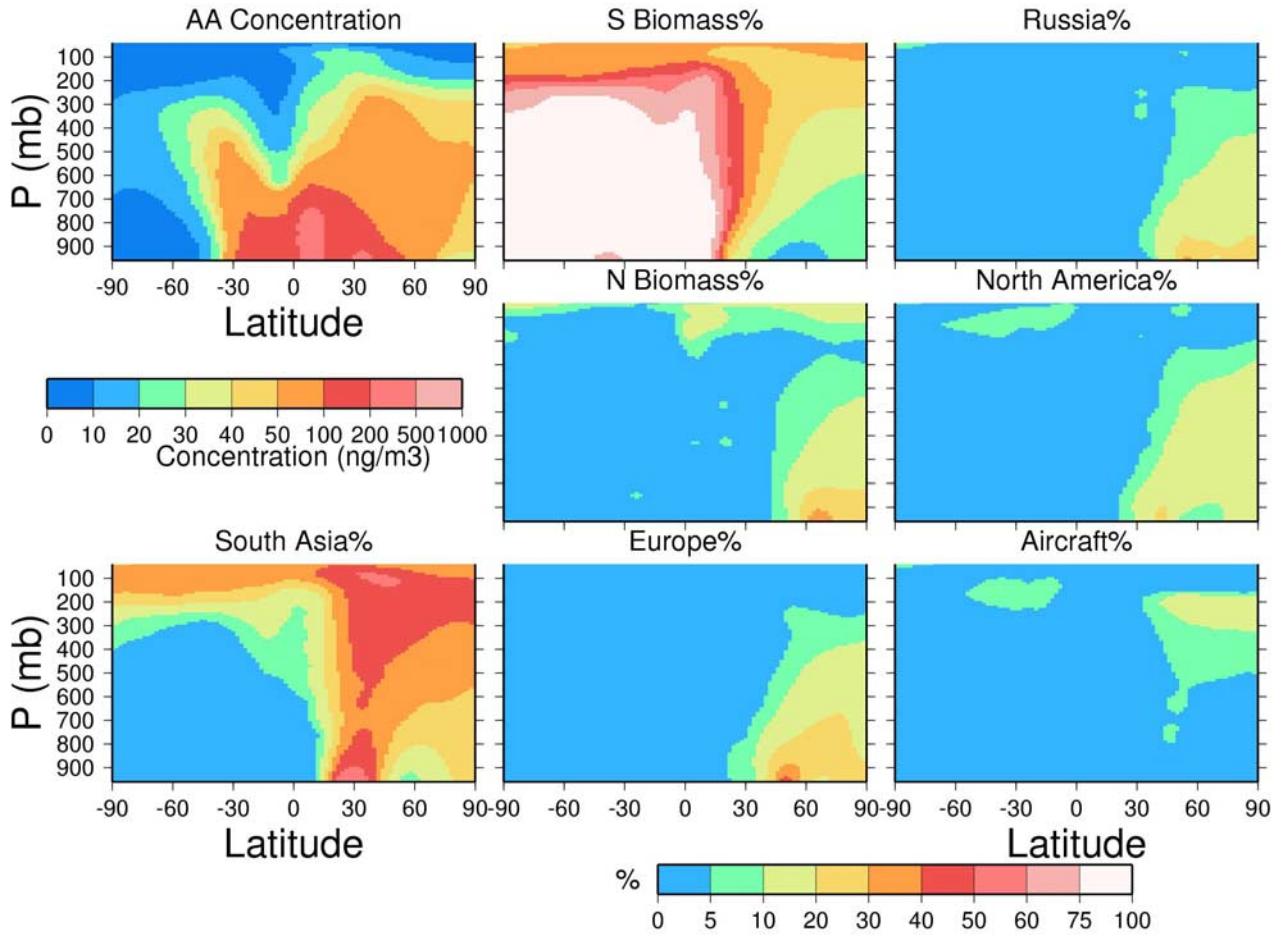

Figure 6. (top left) Annual zonal mean black carbon concentration (ng m^{-3}) and percent contributions from regional experiments.

south Asia, Russia) a longer lifetime results in a greater relative contribution to the burden. Similarly, biomass burning accounts for 56% of the total emission, but contributes 61.3% to the global BC burden. This is due in part to its emission into the full thickness of the boundary layer and in part because of the burning coinciding with dry seasons. Aircraft emissions appear to be negligible, however they do make a small contribution to the burden since they are emitted primarily above clouds. BC aerosols emitted in Europe, North America and "the rest of the world" have relatively shorter lifetimes, and therefore make a relatively smaller contribution to the global burden.

3.2. Annual Mean Column Optical Thickness

[24] Next we consider the impact of various emissions on the annual mean BC optical thickness in the Arctic (Figure 4). According to the model, the BC optical thickness is generally between 0.02 and 0.03 throughout the Arctic, except over Greenland where it is less. Most of the load is from south Asia (20–40%) with higher amounts over the western Arctic. Biomass burning from north of 40°N (primarily from Russia, see Figure 1), biomass burning from south of 40°N and industrial emissions from North America, Russia and Europe each contribute 10–20% to the Arctic BC optical thickness.

[25] Note that the largest contribution to the BC optical thickness over the Atlantic is also from south Asia. Since this component is probably above the surface it may correspond to the TARFOX observation that absorbing aerosols increase with altitude [*Novakov et al.*, 1997].

3.3. Arctic Haze: Springtime Transport

[26] The greatest pollution transport near the surface is observed to occur during late winter and early spring, during Arctic haze transport events [e.g., *Barrie*, 1986]. Typically, blocking enables efficient transport northward, and conditions are most favorable over the Atlantic/European region and in the Pacific [*Iversen and Joranger*, 1985]. The optical thickness in January–March (JFM) is compared with the annual mean in Figure 4. The model has largest BC optical thickness during JFM, so that it is about 50% higher for much of the Arctic. However this seasonality is strongest in the eastern Arctic and is weaker in the west.

[27] This winter-spring transport occurs primarily at relatively low altitudes in the model, as reported in the real world. In Figure 5 we show the January–March mean concentration in the lowest three model layers (up to 910 mbar or 1 km). There are substantial contributions from Russia and Europe, as well as south Asia, each making 20–30% of the concentration near the pole. Again we see that a substantial amount, 20–30%, of the BC in the Atlantic is derived from south Asia, even near the surface. Biomass burning makes a small contribution to the surface BC (<10%) in the Arctic because the southern biomass resides

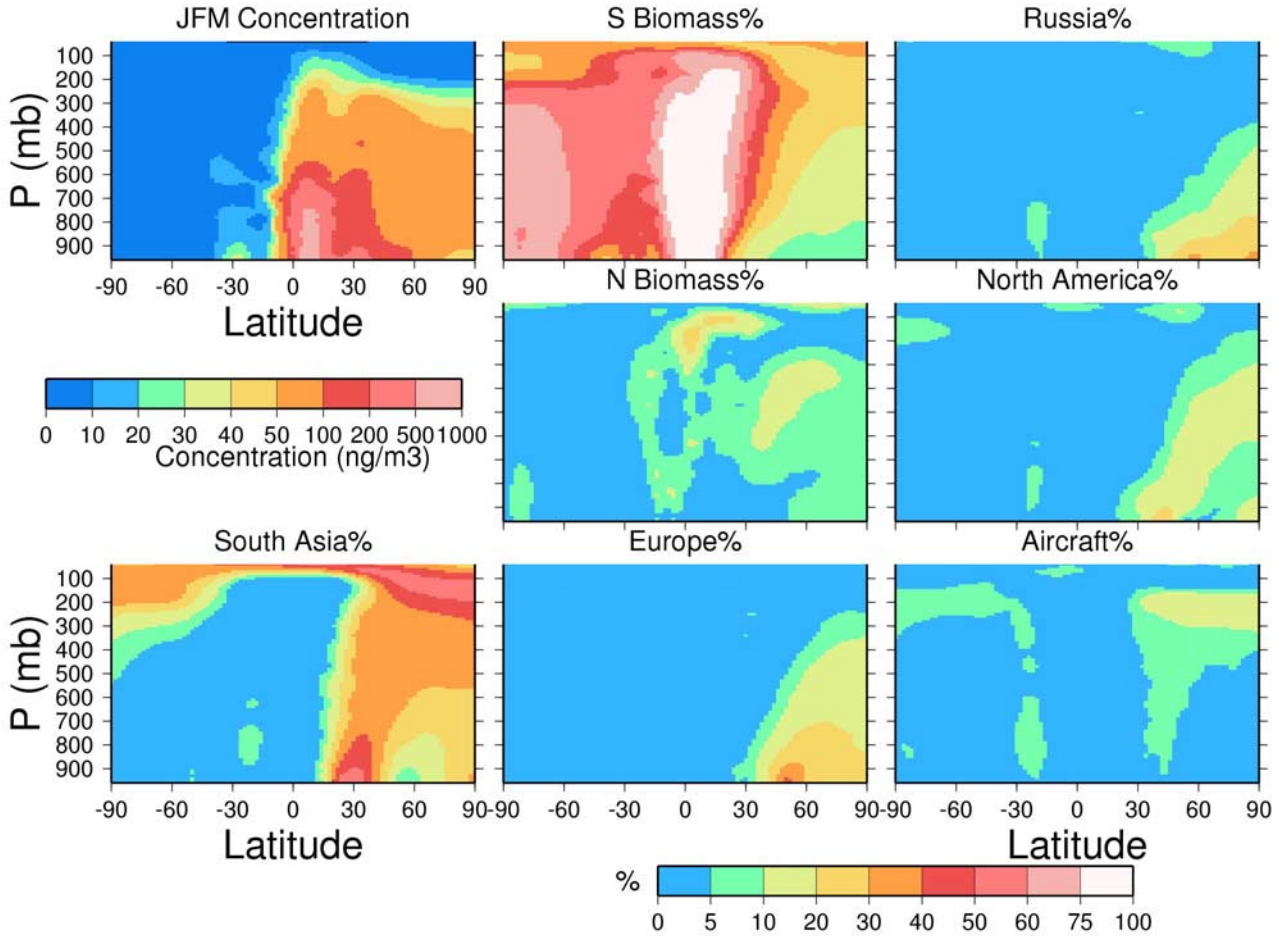

Figure 7. (top left) January–March zonal mean black carbon concentration (ng m^{-3}) and percent contributions from regional experiments.

at higher altitudes and the northern biomass burning is minimal during this season.

3.4. High Altitude: Comparison With Winter Aircraft Data

[28] The vertical distribution of transport to the Arctic can be seen in the zonal mean Figures 6 (annual mean) and 7 (January–March). Comparing the zonal mean concentrations in Figures 6 and 7, we see an increase in BC concentration during the winter-spring that extends from the surface up to 600 mbar over the pole.

[29] As already shown, the largest contributions near the surface in the winter-spring are from Russia, Europe and south Asia. While Europe's and Russia's loads decrease with altitude, other source regions increase with altitude. In the annual mean, the largest contributions near the surface are from northern biomass burning and Eurasia, with the south Asian contribution being largest in the column.

[30] Lofting by convection and the general circulation over the continents enables the long-range transports from the southern biomass regions and Asia. However the seasonal maximum in winter-spring of BC over the Arctic is derived primarily from low-level advection of European and Russian emissions.

[31] In order to assess the model's ability to simulate high altitude BC we compare with the aircraft data of *Baumgardner et al.* [2004] collected in January–February 2003 in the upper troposphere/lower stratosphere (UT/LS) in the high latitudes of the Atlantic. In Figure 8 we show a scatterplot of the aircraft data and corresponding model values. Also shown are the observation values and the model bias. The observations, which are instantaneous aircraft measurements, have much greater variability, with high concentrations tending to occur in the vicinity of Greenland and over the pole. The model (mean of January–February) has a nearly constant value at these altitudes, mostly within layers 9 and 10 of the model. As a result, the model tends to be too high in the regions where the measurements show low values, and agrees better in the high concentration regions. Note that most of these observations were taken from the lower stratosphere. This model appears to have excessive vertical transport and stratosphere-troposphere exchange, on the basis of comparison of modeled and observed aerosol radionuclides in the stratosphere (Koch et al., submitted manuscript, 2005). This may explain in part the excessive BC that we see here.

[32] Figure 9 shows the average model concentration in model layers 9 and 10, along with the regional contributions, for January, February and March. We see that at this

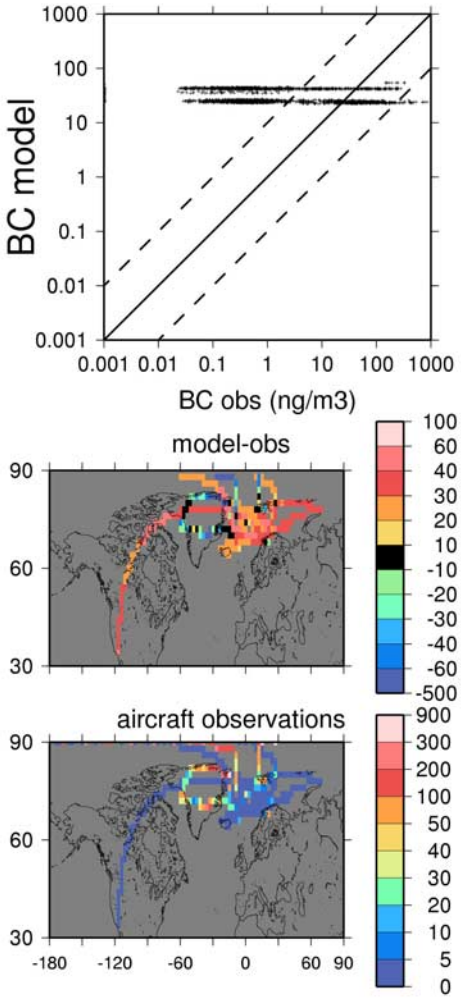

Figure 8. Comparison of model and aircraft data of *Baumgardner et al.* [2004]: (top) scatterplot comparison, (middle) difference between model and observations, and (bottom) observations. Units are ng m^{-3}, and model is the average of January–February.

altitude (approximately 300–150 mbar) the largest source of BC is from south Asia (40–50%), followed by southern biomass burning (20–30%), aircraft emissions (10–20%) and North America (5–10%). The BC from Russia and Europe does not make it high enough to contribute significantly (see Figure 7).

3.5. Deposition on Greenland

[33] The BC deposited on Greenland is derived primarily from the dry and wet deposition of the BC near the surface. Figure 10 shows the annual mean deposition flux and the percentage that is dry deposited. Not surprisingly, the dry deposition makes a greater contribution in dry regions. According to the model, Greenland receives most (60–75%) of its BC from dry deposition. This contrasts with *Davidson et al.* [1985, 1987] who estimated 10–30% dry deposition on Greenland for sulfate, although these estimates are highly uncertain. Furthermore, BC is probably less soluble than sulfate and therefore should have higher dry deposition percent. On the other hand, scavenging by snow is very poorly known, and could be greater than what we assume here (we use the same scavenging rate as below liquid water clouds).

[34] The percentage diagrams of BC deposition in the Arctic (Figure 10) can best be interpreted by comparing with the annual zonal mean Figure 6. The Arctic deposition percentages are comparable to the concentration percentages in the lowest 300 mbar north of 70° as seen in Figure 6. Most deposition is from these lower altitudes. Note also that Arctic drizzle is maximum during summertime and that the northern biomass burning is maximum during summer and fall, thus we see a very substantial contribution to Arctic BC deposition coming from northern biomass burning.

[35] The model indicates that the largest contribution to BC deposited on Greenland is from south Asia (20–30%), with nearly as much coming from Europe. North America and northern biomass burning contribute 10–20% each. Russia contributes at least 10% over the western portion of Greenland.

3.6. Radiative Impacts

[36] Figure 11 shows the annual mean top of the atmosphere instantaneous radiative forcing by the BC aerosols, including the contributions from individual source regions. These contributions, for the most part, reflect the BC optical thickness (Figure 4). The forcing increases with BC altitude, as aerosols above clouds have greater absorption [*Haywood and Ramaswamy*, 1998]. However, the greater absorption is approximately canceled by reduced effectiveness of absorbing aerosols as a radiative forcing with greater altitude of the aerosols [*Hansen et al.*, 1997]; so a map of BC absorption is a good measure of the effective climate forcing of the absorbing aerosols. Note that the forcing referred to here is the total BC forcing; that is, we have not attempted to subtract the preindustrial biomass forcing to obtain the anthropogenic forcing.

3.7. Arctic Sulfate

[37] Although the focus of this study is BC, we performed parallel experiments for sulfate, distinguishing between industrial contributions from the same regions as for BC. Our model and emissions are described by Koch et al. (submitted manuscript, 2005). The industrial SO_2 emission for the year 2000 is based on IIASA (International Institute for Applied Systems Analysis) energy use statistics combined with results from the RAINS (Regional Air Pollution and Simulation) model [e.g., *Amann et al.*, 1999] and the EDGAR 3.2 (1995) emissions (http://www.rivm.nl/edgar). This emission data set has been compiled for the AEROCOM model intercomparison by Frank Dentener and colleagues (available at http://nansen.ipsl.jussieu.fr/AEROCOM). The industrial emissions are isolated according to the regions shown in Figure 1, however we do not isolate the biomass burning contribution; the SO_2 from biomass is small. In Table 2 we show the percent of the industrial emissions from each region and the percent contribution to the annual mean Arctic optical thickness from each region. The same quantities for BC are provided for comparison. For sulfate, Russia contributes most to the optical thickness. This is because Russian sulfur emissions are estimated to be relatively greater (compared with BC).

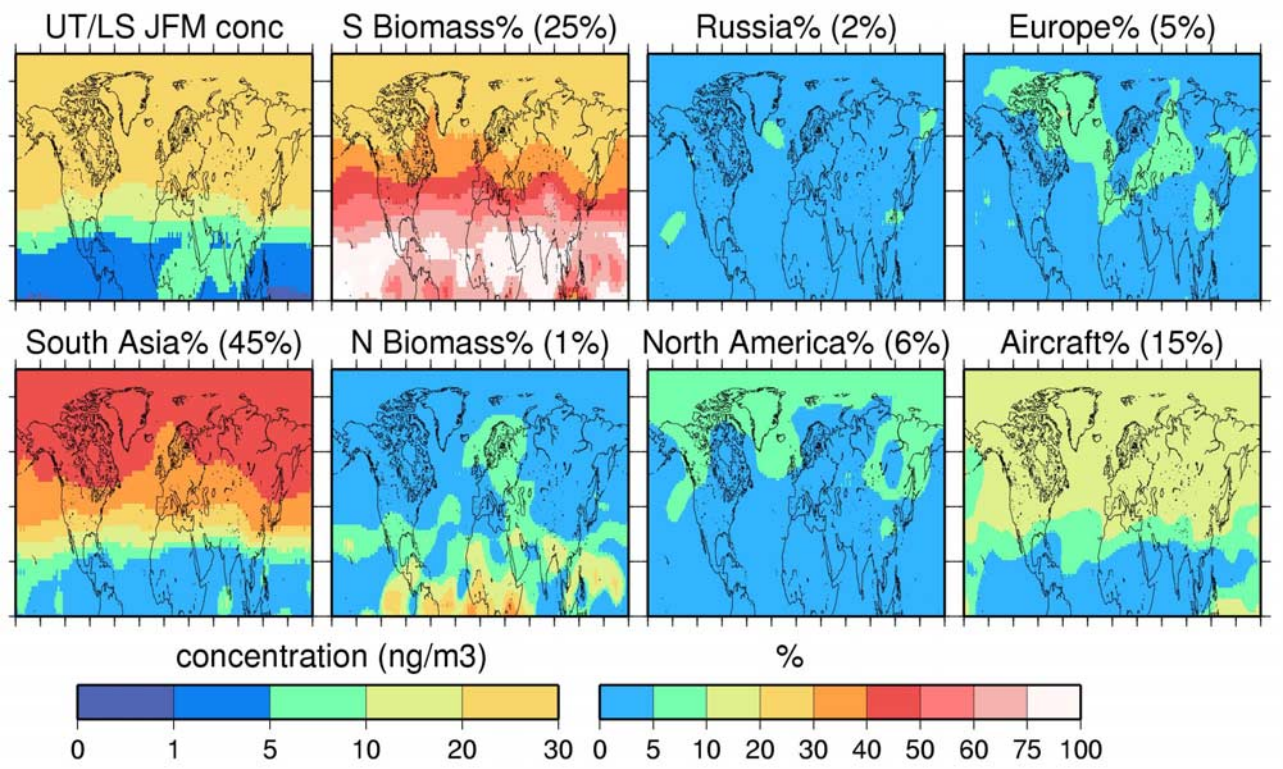

Figure 9. Model BC concentration in layers 9 and 10 (247 and 180 mbar), where the observations of *Baumgardner et al.* [2004] were taken (ng m^{-3}) and percent contributions from the regional experiments. Numbers in parentheses are average percent contribution to BC concentration in $L = 9$, 10 in the Arctic.

Conversely, sulfur emissions from south Asia are less compared with BC and therefore the contribution to the Arctic optical thickness is less, although again substantial.

[38] An interesting coincidence is that, for both BC and sulfate, these 4 region contributions total up to about 70% of the Arctic optical thickness, with the remaining 30% coming from other sources. For BC we have seen that the remainder is mostly from biomass. For sulfate, the remainder would come primarily from natural emissions such as DMS and volcanoes.

4. Discussion

[39] Our global model indicates that most of the black carbon in the present-day Arctic comes from industrial and biofuel sources in south Asia and from biomass burning. Such BC arrives in the Arctic at higher altitudes throughout the year, in contrast with the surface-level springtime haze that is often the focus of Arctic haze studies. We do not imply that most of the BC in these distant regions is transported to the Arctic. On the contrary, according to our model most of south Asian BC remains south of 60°N. However enough of it makes its way north to become the major contributor to Arctic BC, so that about 20–40% of Arctic BC optical thickness comes from south Asia. This region has the largest industrial BC emission, about 21% of the global emission. It contributes about 20% to the lower troposphere winter-spring transport to the Arctic, or Arctic haze, and to surface deposition. Because the south Asian BC tends to travel at higher altitudes, it contributes a higher percentage to optical thickness and radiative forcing (20–40%).

[40] BC emissions from southern (<40°N) biomass burning have a similar story. Again, most of these biomass emissions remain at low latitudes and contribute to the BC load there. However, enough of the BC is lofted to higher altitudes, according to the model, to make significant contributions to the Arctic burden. About 60% of the global BC is from southern biomass burning. In the Arctic it contributes substantially to optical thickness and radiative forcing (10–20%).

[41] In this study we have distinguished between biomass and industrial emissions. If we had combined these, we would have found comparable contributions from south Asia and Russia, since most of the northern biomass burning emissions are from Russia. Thus, as seen in Figure 4, the total Russian contribution to the annual mean optical thickness is about 30%, similar to that from south Asia. However the northern biomass burning is maximum during summer and fall and thus generally should not contribute significantly to the springtime Arctic haze.

[42] We have assumed the "climatological" biomass burning emissions inventory of *Cooke and Wilson* [1996]. We note that it does not include biomass burning from China, and is thus lacking at least 1/4 of Asian biomass (according to the year 2000 estimates of *Streets et al.* [2003]). Also we note that there is considerable interannual variability for Russian biomass burning [*Duncan et al.*, 2003]. Thus the contribution of northern biomass to the

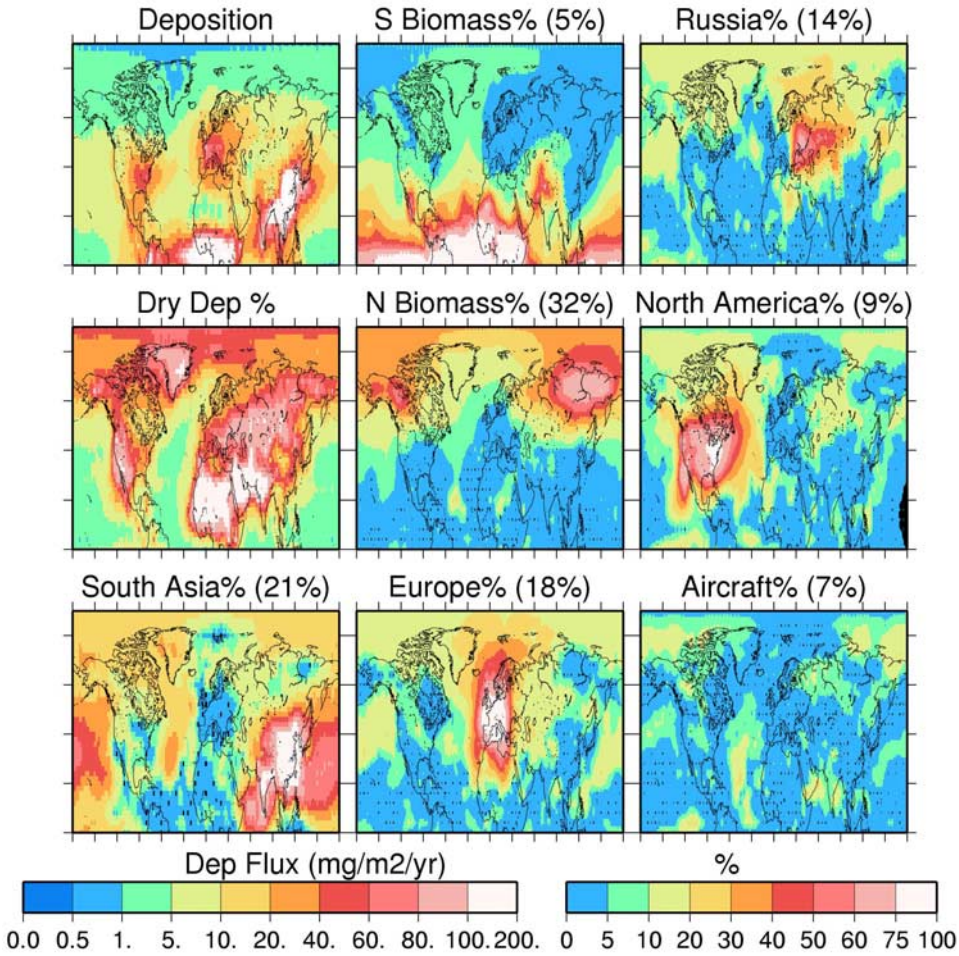

Figure 10. (top left) Annual mean deposition flux, (middle left) percent of total deposition from dry deposition, and percent contributions from regional experiments. Numbers in parentheses are average percent contribution to BC deposition flux in the Arctic.

Arctic should also vary, and this could cause interannual variability in Arctic BC.

[43] Sulfur industrial emissions are distributed differently than BC, with relatively less coming from south Asia and more from Russia. The model indicates that Russia makes the greatest contribution to Arctic sulfate optical thickness (24%), followed by south Asia (17%), Europe (14%) and North America (13%). The prominent role of Russian sulfur emissions is consistent with many Arctic haze studies. However, the SO_2 from south Asia again makes a substantial contribution to Arctic aerosol pollution. Note that at the peak of Russian industrial activity, that is, 2–3 decades ago, Russian emissions would have contributed more of both sulfate and BC.

[44] The distant sources are generally not considered in studies of pollution in the Arctic. This may be because their contribution to the surface level winter-spring Arctic haze is less than that of Europe and Russia. Transport from south Asia tends to occur at higher altitudes and for a greater portion of the year than traditionally assumed for Arctic haze. In addition, the long-distance transport from south Asia and southern biomass regions may take longer, further limiting these distant sources from trajectory analysis.

[45] Our results are consistent with other studies that suggest a large amount of Arctic pollutants, especially black carbon, travels to the Arctic at high altitudes. Arctic aircraft observations [e.g., *Hopper et al.*, 1994; *Raatz et al.*, 1985] found BC to increase with altitude in many regions of the Arctic. The Northern Atlantic, which appears in our model to be downwind of the Arctic BC from south Asia (Figure 4), also appears to have increasing carbonaceous material with altitude [*Novakov et al.*, 1997].

[46] Carbonaceous aerosols are notoriously difficult to simulate and our results consequently come with caveats. The model tends to underestimate BC concentrations near source regions and overestimate concentrations in more remote regions. This is consistent with the findings of *Sato et al.* [2003], who found BC absorption in 2 models to be lower by a factor of 2–4 compared to AERONET observations, which are predominantly located near source regions. The cause of the discrepancy is still not understood. *Sato et al.* [2003] estimated that a factor of two in excess BC absorption may be a result of internal mixing of aerosols rather than a BC mass deficiency, but this would not fully explain the observed BC absorption. Perhaps the emissions are too small and model lifetimes too long. In any case, it may be that this causes an exaggerated transport from the

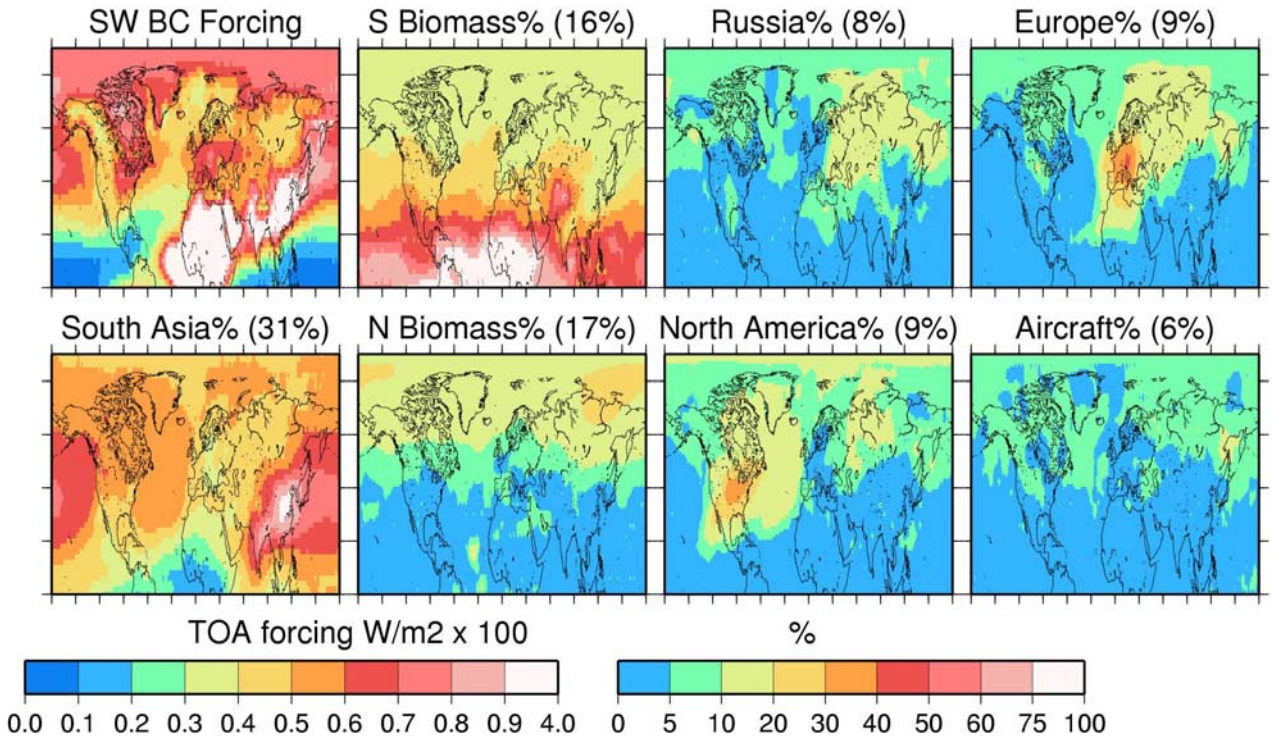

Figure 11. (top left) Annual mean instantaneous top of the atmosphere radiative forcing and percent of forcing from regional experiments. Numbers in parentheses are average percent contribution to BC shortwave forcing in the Arctic.

distant south Asia and southern biomass regions to the Arctic. The model overestimates the concentrations in the upper troposphere and lower stratosphere, again pointing to excessive contributions from south Asia and southern biomass, which dominate the burden there.

[47] Despite the possibility that the model exaggerates long-range transport of aerosols, our results suggest that these distant source regions are probably significant contributors to Arctic BC abundance. The existence of substantial contribution from distant sources is supported by observations such as large BC amount at midlevels of the troposphere, so there is evidence supporting a prominent role for southeast Asian sources in the Arctic. The timing and location of Arctic warming and sea ice loss in the late 20th century is consistent with south Asian sources. According to *Baumgardner et al.* [2004], BC concentrations in the UT/LS over the Arctic seem to have doubled between 1980 and 1995 (although they also indicate that the early data are highly uncertain). BC emissions from developed countries have declined and aircraft are apparently not to blame. However, during this time BC emissions from China and India have nearly doubled [*Novakov et al.*, 2003]. Also, the model indicates that most of the concentrations in this region of the UT/LS are from south Asia.

[48] According to the 2002 AMAP Assessment [*MacDonald et al.*, 2003], the past three decades show significant decreases in sea ice thickness and extent. This recent decrease is greatest in spring and fall and occurs in the western Arctic (western North America and Siberia). These observations defy recent modeling efforts, which show the largest impact of increased CO_2 on the Arctic winter rather than summer [*MacDonald et al.*, 2003]. The pattern of sea ice loss is believed to be linked to the phase of the AO [*MacDonald et al.*, 2003]. However it is interesting that these decades correspond to the increases in BC from south Asia, and that this BC is transported over the Pacific and into the western Arctic, during summer as well as spring. Prior to this, sea ice also decreased during the 1930s–1940s. However this occurred during winter in the eastern part of the Arctic. Again it is interesting to note that during this earlier period, pollution from coal burning in the United States, Europe and Russia [*Novakov et al.*, 2003] would have been transported to the Arctic during winter-spring, and the Eurasian sources would deposit heavily in the eastern Arctic (see Figure 10).

[49] Although our model has considerable uncertainties, we feel the results, together with other lines of evidence, warrant a careful look at the potential impact of south Asia and low-latitude biomass sources on Arctic BC. Studies which associate elements found in the Arctic with various pollution sources should consider these distant sources. For

Table 2. Regional Industrial Emissions and Contribution to Arctic τ

Region	Sulfur Emissions, %[a]	Sulfate Arctic τ, %	BC Emissions, %[a]	BC Arctic τ, %
South Asia	33	17	44	30
Europe	14	14	10	14
North America	16	13	8	11
Russia	10	24	4	12

[a]Percent of global industrial emissions.

example, mercury has been observed to increase in the Arctic and this may be traced to coal burning in Asia [*Macdonald et al.*, 2003]. Trace element studies of emissions from south Asia, along with Europe and Russia should be compared with those in Arctic pollution. Ideally such analysis would be done using aircraft observations, since much of the Arctic BC may never reach the surface but may remain at higher altitudes.

[50] **Acknowledgments.** Support for this research is from the NASA Radiation Science Program and from the NASA Climate Modeling Program. We thank Darrel Baumgardner for sharing his aircraft BC measurements with us. We thank Glenn Shaw for helpful comments on the manuscript.

References

Ackerman, A., O. Toon, D. Stevens, A. Heymsfield, V. Ramanathan, and E. Welton (2000), Reduction of tropical cloudiness by soot, *Science*, *288*, 1042–1047.

Amann, M., J. Cofala, C. Heyes, Z. Klimont, and W. Schoepp (1999), The RAINS model: A tool for assessing regional emission control strategies in Europe, *Pollut. Atmos.*, *4*, 41–63.

Barrie, L. A. (1986), Arctic air pollution: An overview of current knowledge, *Atmos. Environ.*, *20*, 643–663.

Baughcum, S. L., D. M. Chan, S. M. Happenny, S. C. Henderson, P. S. Hertel, T. Higman, D. R. Maggiora, and C. A. Oncina (1993), Emissions scenarios development: Scheduled 1990 and projected 2015 subsonic, Mach 2.0 and Mach 2.4 aircraft, in *The Atmospheric Effects of Stratospheric Aircraft: A Third Program Report*, *NASA Ref. Publ.*, *1313*, 89–131.

Baumgardner, D., G. Kok, and G. Raga (2004), Warming of the Arctic lower stratosphere by light absorbing particles, *Geophys. Res. Lett.*, *31*, L06117, doi:10.1029/2003GL018883.

Bertschi, I. T., D. A. Jaffe, L. Jaeglé, H. U. Price, and J. B. Dennison (2004), PHOBEA/ITCT 2002 airborne observations of transpacific transport of ozone, CO, volatile organic compounds, and aerosols to the northeast Pacific: Impacts of Asian anthropogenic and Siberian boreal fire emissions, *J. Geophys. Res.*, *109*, D23S12, doi:10.1029/2003JD004328.

Biscaye, P. E., F. E. Grousset, A. M. Svensson, A. Bory, and L. Barrie (2000), Eurasian air pollution reaches eastern North America, *Science*, *290*, 2258–2259.

Bodhaine, B. A. (1995), Aerosol absorption measurements at Barrow, Mauna Loa and the South Pole, *J. Geophys. Res.*, *100*, 8967–8976.

Bond, T. C., D. G. Streets, K. F. Yarber, S. M. Nelson, J.-H. Woo, and Z. Klimont (2004), A technology-based global inventory of black and organic carbon emissions from combustion, *J. Geophys. Res.*, *109*, D14203, doi:10.1029/2003JD003697.

Bowling, S. A., and G. E. Shaw (1992), The thermodynamics of pollutant removal as an indicator of possible source areas for Arctic haze, *Atmos. Environ., Part A*, *26*, 2953–2961.

Brock, C. A., L. F. Radke, J. H. Lyons, and P. V. Hobbs (1989), Arctic hazes in summer over Greenland and the North American Arctic. I: Incidence and origins, *J. Atmos. Chem.*, *9*, 129–148.

Cahill, C. F. (2003), Asian aerosol transport to Alaska during ACE-Asia, *J. Geophys. Res.*, *108*(D23), 8664, doi:10.1029/2002JD003271.

Cheng, M.-D., P. K. Hopke, L. Barrie, A. Rippe, M. Olson, and S. Landsberger (1993), Qualitative determination of source regions of aerosol in Canadian high Arctic, *Eviron. Sci. Technol.*, *27*, 2063–2071.

Clarke, A. D., and J. Noone (1985), Measurements of soot aerosol in Arctic snow, *Atmos. Environ.*, *19*, 2045–2054.

Cooke, W. F., and J. J. N. Wilson (1996), A global black carbon model, *J. Geophys. Res.*, *101*, 19,395–19,409.

Davidson, C. I., S. Santhanam, R. C. Fortmann, and M. P. Olson (1985), Atmospheric transport and deposition of trace elements onto the Greenland Ice Sheet, *Atmos. Environ.*, *19*, 2065–2081.

Davidson, C. I., R. E. Honrath, J. B. Kadane, R. S. Tsay, P. A. Mayewski, W. B. Lyons, and N. Z. Heidam (1987), The scavenging of atmospheric sulfate by Arctic snow, *Atmos. Environ.*, *21*, 871–882.

Duncan, B. N., R. V. Martin, A. C. Staudt, R. Yevich, and J. A. Logan (2003), Interannual and seasonal variability of biomass burning emissions constrained by satellite observations, *J. Geophys. Res.*, *108*(D2), 4100, doi:10.1029/2002JD002378.

Hansen, J., and L. Nazarenko (2004), Soot climate forcing via snow and ice albedos, *Proc. Natl. Acad. Sci. U. S. A.*, *101*, 423–428, doi:10.1073/pnas.2237157100.

Hansen, J., and M. Sato (2001), Trends of measured climate forcing agents, *Proc. Natl. Acad. Sci. U. S. A.*, *98*, 14,778–14,783, doi:10.1073/pnas.261553698.

Hansen, J., M. Sato, and R. Ruedy (1997), Radiative forcing and climate response, *J. Geophys. Res.*, *102*, 6831–6864.

Hansen, J., et al. (2002), Climate forcings in Goddard Institute for Space Studies SI2000 simulations, *J. Geophys. Res.*, *107*(D18), 4347, doi:10.1029/2001JD001143.

Harris, J. M., and J. D. W. Kahl (1994), Analysis of 10-day isentropic flow patterns for Barrow, Alaska: 1985–1992, *J. Geophys. Res.*, *99*, 25,845–25,855.

Haywood, J., and V. Ramaswamy (1998), Global sensitivity studies of the direct radiative forcing due to anthropogenic sulfate and black carbon aerosols, *J. Geophys. Res.*, *103*, 6043–6058.

Hodges, G. (2000), The new cold war: Stalking Arctic climate change by submarine, *Natl. Geogr.*, *201*(3), 30–41.

Hopper, J. F., D. E. J. Worthy, L. A. Barrie, and N. B. A. Trivett (1994), Atmospheric observations of aerosol black carbon, carbon dioxide, and methane in the high Arctic, *Atmos. Environ.*, *28*, 3047–3054.

Huebert, B., T. Bertram, J. Kline, S. Howell, D. Eatough, and B. Blomquist (2004), Measurements of organic and elemental carbon in Asian outflow during ACE-Asia from the NSF/NCAR C-130, *J. Geophys. Res.*, *109*, D19S11, doi:10.1029/2004JD004700.

Intergovernmental Panel on Climate Change (1999), *Aviation and the Global Atmosphere*, edited by J. E. Petter et al., Cambridge Univ. Press, New York.

Iversen, T., and E. Joranger (1985), Arctic air pollution and large scale atmospheric flows, *Atmos. Environ.*, *19*, 2099–2108.

Jacobson, M. (2001), Strong radiative heating due to the mixing state of black carbon in atmospheric aerosols, *Nature*, *409*, 695–697.

Kaneyasu, N., and S. Murayama (2000), High concentrations of black carbon over middle latitudes in the North Pacific Ocean, *J. Geophys. Res.*, *105*, 19,881–19,890.

Khattatov, V. U., A. E. Tyabotov, A. P. Alekseyev, A. A. Postnov, and E. A. Stulov (1997), Aircraft lidar studies of the Arctic haze and their meteorological interpretation, *Atmos. Environ.*, *44*, 99–111.

Klonecki, A., P. Hess, L. Emmons, L. Smith, J. Orlando, and D. Blake (2003), Seasonal changes in the transport of pollutants into the Arctic troposphere-model study, *J. Geophys. Res.*, *108*(D4), 8367, doi:10.1029/2002JD002199.

Koch, D. (2001), Transport and direct radiative forcing of carbonaceous and sulfate aerosols in the GISS GCM, *J. Geophys. Res.*, *106*, 20,311–20,332.

Lamarque, J.-F., and P. G. Hess (2003), Model analysis of the temporal and geographical origin of the CO distribution during the TOPSE campaign, *J. Geophys. Res.*, *108*(D4), 8354, doi:10.1029/2002JD002077.

Liang, Q., L. Jaeglé, D. A. Jaffe, P. Weiss-Penzias, A. Heckman, and J. A. Snow (2004), Long-range transport of Asian pollution to the northeast Pacific: Seasonal variations and transport pathways of carbon monoxide, *J. Geophys. Res.*, *109*, D23S07, doi:10.1029/2003JD004402.

Liousse, C., J. E. Penner, C. Chuang, J. J. Walton, H. Eddleman, and H. Cachier (1996), A global three-dimensional model study of carbonaceous aerosols, *J. Geophys. Res.*, *101*, 19,411–19,432.

Lowenthal, D. H., and R. D. Borys (1997), Sources of pollution aerosol at Dye 3, Greenland, *Atmos. Environ.*, *22*, 3707–3717.

Lowenthal, D. H., and K. A. Rahn (1985), Regional sources of pollution aerosol at Barrow, Alaska during winter 1979–80 as deduced from elemental tracers, *Atmos. Environ.*, *19*, 2011–2024.

Macdonald, R. W., T. Harner, J. Fyfe, H. Loeng, and T. Weingartner (2003), *AMAP Assessment 2002: The Influence of Global Change on Contaminant Pathways to, Within, and From the Arctic*, 65 pp., Arct. Monit. and Assess. Program., Oslo.

Manabe, S., M. M. Spelman, and R. J. Stouffer (1992), Transient responses of a coupled ocean-atmosphere model to gradual changes in atmospheric CO_2, *J. Clim.*, *5*, 105–126.

Matsuki, A., et al. (2003), Seasonal dependence of the long-range transport and vertical distribution of free tropospheric aerosols over east Asia: On the basis of aircraft and lidar measurements and isentropic trajectory analysis, *J. Geophys. Res.*, *108*(D23), 8663, doi:10.1029/2002JD003266.

Novakov, T., D. A. Hegg, and P. Hobbs (1997), Airborne measurements of carbonaceous aerosols on the east coast of the United States, *J. Geophys. Res.*, *102*, 30,023–30,030.

Novakov, T., V. Ramanathan, J. E. Hansen, T. W. Kirchstetter, M. Sato, J. E. Sinton, and J. A. Sathaye (2003), Large historical changes of fossil-fuel black carbon aerosols, *Geophys. Res. Lett.*, *30*(6), 1324, doi:10.1029/2002GL016345.

Perry, K. D., T. A. Cahill, R. C. Schnell, and J. M. Harris (1999), Long-range transport of anthropogenic aerosols to the National Oceanic and Atmospheric Administration baseline station at Mauna Loa Observatory, Hawaii, *J. Geophys. Res.*, *104*, 18,521–18,533.

Raatz, W. E. (1985), Meteorological conditions over Eurasia and the Arctic contributing to the March 1983 Arctic haze episode, *Atmos. Environ.*, *19*, 2121–2126.

Raatz, W. E., R. C. Schnell, B. A. Bodhaine, S. J. Oltmans, and R. H. Gammon (1985), Air mass characteristics in the vicinity of Barrow, Alaska, 9–19 March 1983, *Atmos. Environ.*, *19*, 2127–2134.

Rahn, K. A. (1981a), Relative importances of North America and Eurasia as sources of Arctic aerosol, *Atmos. Environ.*, *15*, 1447–1455.

Rahn, K. A. (1981b), The Mn/V ratio as a tracer of large-scale sources of pollution aerosol for the Arctic, *Atmos. Environ.*, *15*, 1457–1464.

Rahn, K. A., and D. H. Lowenthal (1984), Elemental tracers of distant regional pollution aerosols, *Science*, *223*, 132–139.

Rahn, K. A., R. D. Borys, and G. E. Shaw (1977), The Asian source of Arctic haze bands, *Nature*, *268*, 713–715.

Rinke, A., K. Dethloff, and M. Fortmann (2004), Regional climate effects of Arctic haze, *Geophys. Res. Lett.*, *31*, L16202, doi:10.1029/2004GL020318.

Rosen, H., and A. D. A. Hansen (1984), Role of combustion-generated carbon particles in the absorption of solar radiation in the Arctic haze, *Geophys. Res. Lett.*, *11*, 461–464.

Sato, M., J. Hansen, D. Koch, A. Lacis, R. Ruedy, O. Dubovik, B. Holben, M. Chin, and T. Novakov (2003), Global atmospheric black carbon inferred from AERONET., *Proc. Natl. Acad. Sci. U. S. A.*, *100*, 6319–6324, doi:10.1073/pnas.0731897100.

Scheuer, E., R. W. Talbot, J. E. Dibb, G. K. Seid, L. Debell, and B. Lefer (2003), Seasonal distributions of fine aerosol sulfate in the North American Arctic basin during TOPSE, *J. Geophys. Res.*, *108*(D4), 8370, doi:10.1029/2001JD001364.

Sharma, S., D. Lavoue, H. Cachier, L. A. Barrie, and S. L. Gong (2004), Long-term trends of the black carbon concentrations in the Canadian Arctic, *J. Geophys. Res.*, *109*, D15203, doi:10.1029/2003JD004331.

Shaw, G. E. (1995), The Arctic haze phenomenon, *Bull. Am. Meteorol. Soc.*, *76*, 2403–2413.

Stohl, A., S. Eckhardt, C. Forster, P. James, and N. Spichtinger (2002), On the pathways and timescales of intercontinental air pollution transport, *J. Geophys. Res.*, *107*(D23), 4684, doi:10.1029/2001JD001396.

Streets, D. G., et al. (2003), An inventory of gaseous and primary aerosol emissions in Asia in the year 2000, *J. Geophys. Res.*, *108*(D21), 8809, doi:10.1029/2002JD003093.

VanCuren, R. A. (2003), Asian aerosols in North America: Extracting the chemical composition and mass concentration of the Asian continental aerosol plume from long-term aerosol records in the western United States, *J. Geophys. Res.*, *108*(D20), 4623, doi:10.1029/2003JD003459.

VanCuren, R. A., and T. A. Cahill (2002), Asian aerosols in North America: Frequency and concentration of fine dust, *J. Geophys. Res.*, *107*(D24), 4804, doi:10.1029/2002JD002204.

Vorosmarty, C. J., L. D. Hinzman, B. J. Peterson, D. H. Bromwich, L. C. Hamilton, J. Morison, V. E. Romanovsky, M. Sturm, and R. S. Webb (2001), *The Hydrologic Cycle and Its Role in the Arctic and Global Environmental Change: A Rationale and Strategy for Synthesis Study*, 84 pp., Arct. Res. Consortium of the U.S., Fairbanks, Alaska.

Wallace, J. M., and D. W. J. Thompson (2002), Annular modes and climate prediction, *Phys. Today*, *57*(8), 28–33.

Wilkening, K. E., L. A. Barrie, and M. Engle (2000), Trans-Pacific air pollution, *Science*, *290*, 65–66.

J. Hansen and D. Koch, NASA Goddard Institute for Space Studies, Columbia University, 2880 Broadway, New York, NY 10025, USA. (dkoch@giss.nasa.gov)